Politecnico di Milano
M.Sc. in Mathematical Engineering
Bayesian statistics
Professor A. Guglielmi
AY 2020/2021

Bayesian clustering of functional data

Ajroldi Niccolò
Bortolotti Teresa
Marchionni Edoardo

Contents

1 Introduction

1.1 Data set presentation

Our data come from a study conducted by two hospital units in Provincia di Treviso, Italy; in particular, from Unità Gravi Cerebrolesioni Acquisite of Ospedale Ca' Foncello in Treviso and Unità Gravi Cerebrolesioni e Miolesioni of Ospedale Riabilitativo di Alta Specializzazione in Motta di Livenza.

Population in study is composed of 26 patients, who underwent two stages of assessment of their levels of functionality: first a neurophysiological evaluation while in a coma status and under sedation, and then a recovery evaluation.

During the first stage of the study, patients have been subjected to a stimulation of the median nerve through a needle electrode to the wirst. Somatosensory evoked potentials, which are the electrical modifications occurring in the central nervous system following the stimulus, are detected within 2 seconds after the stimulus.
Detections of the evoked potential have been made in four different positions of the scalp, two frontal and two central, in order to measure its components: SLSEP - Short Latency Somatosensory Evoked Potential and PMLSEP - Pain-related Middle Latency Somatosensory Evoked Potential.
For each patient, we are hence given with four components of the evoked potential, which are PML and SL measured both on the left and on the right of the skull. We performed the analysis considering only one of these components, in particular the SL component measured by the electrode placed on the left lobe.
This component is treated as a functional datum, evaluated in 1600 time points.

After leaving the coma state, patients underwent a period of rehabilitation, at the end of which their levels of recovery have been evaluated and considered with respect to three different scales:

- GOSE_0 - *Glasgow Outcome Scale Extended*, for the assessment of the functional outcome of the patient, with a focus on the independence of the patient in his everyday life. Low levels indicate a negative outcome, high levels indicate a positive outcome.
- LCF_0 - *Level of Cognitive Functioning*, for the assessment of the level of responsiveness of the subject, through a definition of the progression of the recovery. Low levels indicate a negative outcome, high levels indicate a positive outcome.
- DRS_0 - *Disability Rate Scale*, for the assessment of the aspects related to the handicap. Low levels indicate a positive outcome, high levels indicate a negative outcome.

Given the numerosity of patients in the study, indexes of the assessment of the outcome have been syntesized as follows:

- if $\text{GOSE}_0 \leq 4$ then $\text{GOSE} = 1$, if $\text{GOSE}_0 > 4$ then $\text{GOSE} = 2$
- if $\text{LCF}_0 \leq 5$ then $\text{LCF} = 1$, if $\text{LCF}_0 > 5$ then $\text{LCF} = 2$
- if $\text{DRS}_0 \geq 6$ then $\text{DRS} = 1$, if $\text{DRS}_0 < 6$ then $\text{DRS} = 2$

The observed sample did not show any empirical evidence in favor of the hypothesis that index GOSE is associated to indexes DRS or LCF.

1.2 Research question

The analysis aims at performing clustering of functional observations of Somatosensory evoked potential, and investigate the presence of patterns in the levels of recovery of patients, when they are assigned to different clusters.

2 The model

The main purpose is to cluster functional data at our disposal, tackling the problem in a univariate setting. In order to pursue this task we introduce the following model.
First, observed curves $x_1(t), ..., x_n(t)$ are supposed to be realizations of random functions $X_1(t), ..., X_n(t)$ over some suitable space $(\mathcal{X}, \mathcal{B}(\mathcal{X}))$.
We assume that the probability distribution of the observations is represented by a mixture model.
Let $X_i \sim f$, then

$$f(x) = \int_{\Theta} k(x, \theta) p(\delta\theta) \tag{1}$$

where probability p is a random probability measure that follows a Dirichlet Process and $\{k(\cdot, \theta)\}_\theta$ are kernels depending on some parameter $\theta \in \Theta$.
Since Dirichlet Processes are almost sure discrete, the mixture can be reformulated as an infinite sum

$$f(x) = \sum_{i=1}^{\infty} k(x, \theta_i) p_i \tag{2}$$

where the weights p_i sum up to 1 almost surely.

In particular, we assume that the kernels of the mixture are Gaussian processes, where both the mean and the covariance operators play the role of the parameter θ.
This leads us to recast our problem as follows

$$\begin{aligned} X_i|\mu_i, R_i &\overset{ind}{\sim} GP(\mu_i, R_i) \\ (\mu_i, R_i)|G &\overset{iid}{\sim} G \\ G &\sim DP(\alpha, \tilde{H}) \end{aligned} \tag{3}$$

where μ_i is the mean function and R_i is the covariance operator of the Gaussian process.

2.1 Dimensionality reduction

To handle our model and to simulate from the above Dirichlet Process, we have to reduce the dimensionality of the latent random variables. For this purpose each functional observation is assumed to be the sum of two elements

$$X(t) = \mu(t) + \varepsilon \tag{4}$$

where $\mu(t)$ is a function representing a mean effect and $\varepsilon \sim GP(0, R)$ is a stochastic process representing a variance effect.

2.1.1 Covariance operator

Regarding the covariance operator, we assume the following representation

$$R(t, t') = \begin{cases} \phi_t & \text{if } t = t' \\ 0 & \text{if } t \neq t' \end{cases} \tag{5}$$

2.1.2 Mean operator

As far as the mean function is concerned, inspired by Scarpa and Dunson 2014, we resort to a representation on a basis system. Let $\{b_l(t)\}_{l=1,\dots,L}$ be that basis and assume it exactly spans the space $\mathcal{X}$. This allows us to represent any observation as

$$X(t) = \sum_{l=1}^{L} \beta_l b_l(t) \qquad \forall\ t. \tag{6}$$

Defining $\boldsymbol{\beta} = [\beta_1, \dots, \beta_L]^T$ and $\boldsymbol{b}(t) = [b_1(t), \dots, b_l(t)]^T$, we get the more compact representation

$$X(t) = \boldsymbol{\beta}^T \boldsymbol{b}(t) \qquad \forall\ t. \tag{7}$$

In this framework the mean operator μ of each observation can be expanded as follows

$$\mu(t) = \sum_{l=1}^{L} \mu_l b_l(t) \qquad \forall\ t. \tag{8}$$

As above, defining the vector $\boldsymbol{\mu} = [\mu_1, ..., \mu_L]^T$ we can get the more compact representation

$$\mu(t) = \boldsymbol{\mu}^T \boldsymbol{b}(t) \qquad \forall\ t.. \tag{9}$$

From now on, we can refer to $\mu(t)$ and $X(t)$ by means of their random coefficients $\boldsymbol{\mu} := [\mu_1, ..., \mu_L]^T$ and $\boldsymbol{\beta} := [\beta_1, ..., \beta_L]^T$ respectively.

Thanks to the above assumptions, we obtain the following simpler representation of the mixture model:

$$\begin{aligned} X_i|\boldsymbol{\mu}_i, \{\phi_{it}\}_t &\overset{ind}{\sim} GP(\mu_i, R_i) \\ (\boldsymbol{\mu}_i, \{\phi_{it}\}_t)|G &\overset{iid}{\sim} G \\ G &\sim DP(\alpha, H) \end{aligned} \tag{10}$$

2.2 Base measure specification

The Dirichlet Process is a prior over a probability measure and, in order to characterize it, both the mass parameter and the base measure need to be specified. As far as the base measure H is concerned, H is the joint distribution of our latent random variables $(\boldsymbol{\mu}, \{\phi_t\}_t) \sim H$ obtained marginalizing out G.
We assume $\{\phi_t\}_t$ indipendent and identically distributed and $\forall t\ \boldsymbol{\mu} \perp\!\!\!\perp \phi_t$
Under the above assumptions, we can characterize H by specifying the marginal distributions of the latent parameters

$$\boldsymbol{\mu} \sim \mathcal{N}_L(\boldsymbol{m}_0,\ \Lambda_0) \tag{11}$$

$$\phi_t \overset{iid}{\sim} IG(c, d) \tag{12}$$

2.3 Hyperpriors

To get a more sophisticated model and to gain flexibility, we set a hyperprior structure on the parameters of the base measure for $\boldsymbol{\mu}$.

Mean operator
We set a normal-inverse-Wishart distribution on the hyperparameters of the vector $\boldsymbol{\mu}$.
In particular, we set $(\boldsymbol{m}_0,\ \Lambda_0) \sim \text{NIW}(\boldsymbol{\theta_0}, k_0, \nu_0, \Delta_0)$, that has the following hierarchical structure:

$$\begin{aligned}
\boldsymbol{\mu}|\boldsymbol{m_0}, \Lambda_0 &\sim \mathcal{N}(\boldsymbol{m_0}, \Lambda_0) \\
\boldsymbol{m_0}|\Lambda_0 &\sim \mathcal{N}\left(\boldsymbol{\theta_0}, \frac{\Lambda_0}{k_0}\right) \\
\Lambda_0 &\sim \text{IW}(\nu_0, \Delta_0).
\end{aligned}$$

3 Sampling

Our purpose is to sample from the joint posterior distribution of the random probability measure G and parameters. The goal is to perform inference on the latent partition of our observations and on the random density H. In order to do so, we will rely on a Gibbs' sampling algorithm that will be extensively described in the current section.
First, we assume a finite dimensional truncation of the Dirichlet process, with M kernels. This allows us to express the model in terms of a finite number of random variables and to sample from it through a blocked Gibbs sampler.
In this framework, we augment the problem introducing the following random variables:

- $Z_j := (\boldsymbol{\mu}_j, \sigma_j, \{\phi_{jt}\}_t)$, i.e. it denotes the j-*th* kernel-specific latent parameters
- K_i is the assignment categorical variable of our i-*th* datum, it takes values in $\{1, \dots, M\}$ and $K_i = j$ if observation i belongs to the j-*th* kernel
- $Y_j := (\boldsymbol{m_0}_j, \Lambda_{0j})$, i.e. it stands for the j-*th* kernel-specific latent hyperparameter
- p_j is the probability of belonging to the j-*th* kernel, it takes

Furthermore, for the simplicity of notation we introduce the following vectors:

- $\boldsymbol{X}_i := (X_i(t_0), \dots, X_i(T))^T$, where X_i is our i-*th* observation and $t_0, ..., T$ are the time instants at which we observed our data
- $\mathbf{K} := (K_1, \dots, K_n)$
- $\mathbf{Z} := (Z_1, \dots, Z_M)$
- $\mathbf{Y} := (Y_1, \dots, Y_M)$
- $\mathbf{p} := (p_1, \dots, p_M)$

It is noteworthy that the connection with the previous section follows by remarking that $(\boldsymbol{\mu}_i, \{\phi_{it}\}_t) = Z_{K_i}$.
In this context, our model can be rewritten as

$$\begin{aligned}
X_i|\mathbf{Z}, \mathbf{K}, \mathbf{Y} &\overset{ind.}{\sim} \text{Gaussian Process with parameters } Z_{K_i} \\
Z_j|\mathbf{Y} &\overset{iid}{\sim} H \qquad Y_j \overset{iid}{\sim} \mathcal{L} \\
K_i|\mathbf{p} &\overset{iid}{\sim} \text{categorical}(M, \mathbf{p})
\end{aligned} \tag{13}$$

where $j = 1, \dots, M$, $i = 1, \dots, n$ and $\mathbf{p}$ follows a truncated stick breaking construction that will be presented in the next subsection.

3.1 Blocked Gibbs Sampler

The method is a generalization of the algorithm described in Ishwaran and James 2001, it works by iteratively drawing values from the posterior distributions of the blocked variables

$$\begin{gathered}\mathbf{Y}|\mathbf{Z}\\ \mathbf{Z}|\mathbf{K},\mathbf{Y},\mathbf{X}_1,\ldots,\mathbf{X}_n\\ \mathbf{K}|\mathbf{Z},\mathbf{Y},\mathbf{p},\mathbf{X}_1,\ldots,\mathbf{X}_n\\ \mathbf{p}|\mathbf{K}\end{gathered} \tag{14}$$

Each draw $(\mathbf{Z},\mathbf{K},\mathbf{Y},\mathbf{p})$ defines a random probability measure

$$G_M(\cdot)=\sum_{k=1}^{M} p_k\delta_{Z_k}(\cdot), \tag{15}$$

which provides a draw from the posterior $DP(\cdot|\alpha,H,X)$. On the other hand, the allocation variable $\mathbf{K}$ provides a draw of the latent partition induced by the Dirichlet process.
The general idea of the algorithm is to assign, at every iteration, each observation to the most probable group, then draw the hyperparamers from the full conditional for each group and last, conditionally to the observations assigned to the group, draw probable parameters. As an initialization step, we allocate observations to different groups.

Now let $K_1^*,...,K_m^*$ denote the set of current unique values of $\mathbf{K}$.
The blocked Gibbs sampler works iterating the following steps:

1. Draw from the full conditional for $\mathbf{Y}$
2. Draw from the full conditional for $\mathbf{Z}$
3. Draw from the full conditional for $\mathbf{K}$
4. Draw from the full conditional for $\mathbf{p}$

Step 1: conditional for Z
After initialization and after every following iteration, we are given with empty groups and groups to which at least one observation has been assigned.
We distinguish the update rule for these two cases: parameters of an empty group are simulated from the original priors with hyperparameters simulated from the original hyperpriors, while parameters of a non-empty group are drawn from the full conditionals after having drawn the hyperparameters form their full conditionals and hence updated according to the observations assigned to the kernel.

Formally, let $\{K_1^*,...,K_m^*\}$ denote the set of r unique values of K at the current iteration.

For each cluster $j\in\{K_1^*,...,K_m^*\}^c$ (i.e. the empty clusters) simulate

$$\begin{aligned}Y_j &\sim \mathcal{L}\\ Z_j &\sim H(Z_j|Y_j)\end{aligned}$$

For each cluster $j\in\{K_1^*,...,K_m^*\}$ (i.e. the clusters to which at least one observation has been assigned) simulate

$$Y_j|Z_j\sim f(Y_j|Z_j)$$

$$Z_j|\boldsymbol{K},Y_j,X_1,\ldots,X_n\sim f(Z_j|\boldsymbol{K},Y_j,X_1,\ldots,X_n)\propto H(Z_j|Y_j)\prod_{\{i:K_i=j\}} f(X_i|Z_j)$$

Step 2: conditional for K
For each observation i = 1, ..., n do

for every cluster j, evaluate the probability that observation i belongs to cluster j as p_j times the kernel density evaluated in $(\mu_j, \phi_{j1}, \dots, \phi_{jT})$.

The result is a M-dimensional vector of probabilities:

$$\mathbf{p_i} := (p_{1,i}, \dots, p_{M,i}) \propto (p_1 f(X_i|Z_1, Y_1), \dots, p_M f(X_i|Z_M, Y_M)) \tag{16}$$

Simulate $K_i|\mathbf{Z}, \mathbf{Y}, \mathbf{p}, \mathbf{X_1}, \dots, \mathbf{X_n} \sim \text{categorical}(M, \mathbf{p}_i)$.

Step 3: conditional for p

Update the weights for each group.

$$\begin{gathered} p_1 = V_1, \\ p_j = V_j \prod_{l<j} (1 - V_l) \text{ , for } j = 2, \dots, M \\ \text{where } V_j \overset{ind}{\sim} Beta\left(1 + M_j, \alpha + \sum_{l=k+1}^{M} M_l\right) \text{ , for } j = 1, \dots, M-1 \\ V_M = 1 \end{gathered} \tag{17}$$

where M_j is the number of observations i such that $K_i = j$.

3.2 Full conditional derivation

In this section, we rely on two representations of the observations, which are equivalent, as we extensively explained in Section 2.1. Therefore, we will not further justify the usage of these representations here.

3.2.1 Full conditional for latent parameters Z_j

The full conditional density of j-*th* kernel-specific parameters is of the form

$$f(Z_j|\boldsymbol{K}, Y_j, X_1, \dots, X_n) \propto H(Z_j|Y_j) \prod_{\{i:K_i=j\}} f(X_i|Z_j, Y_j) \tag{18}$$

Exploiting the vectors $\{\boldsymbol{X}_i\}_i$ and relying on the properties of Gaussian processes (i.e. multivariate Gaussian marginality), we have

$$f(\boldsymbol{X}_i|Z_j, Y_j) = \prod_{t=t_0}^{T} f(X_i(t)|Z_j, Y_j) = \prod_{t=t_0}^{T} \frac{1}{\sqrt{2\pi\phi_{jt}}} \exp\left\{-\frac{(X_i(t) - \mu_j(t))^2}{2\phi_{jt}}\right\} \tag{19}$$

For the sake of notation convenience, from now on we drop the index j that denotes the kernel membership, keeping in mind that any full conditional is for the parameters of the j-*th* group.

Full conditional for ϕ_t
Fix $t \in \{t_0, \dots, T\}$, we have

$$f(\phi_t|\text{rest}) \propto H(\phi_t) \prod_{\{i:K_i=j\}} f(X_i(t)|Z_j, Y_j). \tag{20}$$

We recall that prior for ϕ_t is $\forall t\ \phi_t \overset{iid}{\sim} IG(c, d)$.

$$\phi_t|\text{rest} \sim \text{inv-gamma}\left(c + \frac{r}{2}, d + \sum_{\{i:K_i=j\}} \frac{(X_i(t) - \mu(t))^2}{2}\right) \tag{21}$$

Refer to section A of the appendix for computations.

Full conditional for $\boldsymbol{\mu}$
We have

$$f(\boldsymbol{\mu}|\text{rest}) \propto H(\boldsymbol{\mu}|Y_j) \prod_{\{i:K_i=j\}} f(\mathbf{X}_i|Z_j, Y_j)$$

For what concerns the first term, we recall that the prior for $\boldsymbol{\mu}$ is $\boldsymbol{\mu} \sim \mathcal{N}_L(\boldsymbol{m_0}, \Lambda_0)$.

We have that the full conditional for $\boldsymbol{\mu}$ is

$$\boldsymbol{\mu}|\text{rest} \sim \mathcal{N}_L(\boldsymbol{m}_r, \Lambda_r) \tag{22}$$

where

$$\boldsymbol{m}_r = \Lambda_r \left(\Lambda_0^{-1}\boldsymbol{m}_0 + \left[\sum_{t=t_0}^{T} \frac{\boldsymbol{b}(t)\boldsymbol{b}(t)^T}{\phi_t}\right] \sum_{\{i:K_i=j\}} \boldsymbol{\beta}_i\right)$$

$$\Lambda_r = \left(\Lambda_0^{-1} + m\left[\sum_{t=t_0}^{T} \frac{\boldsymbol{b}(t)\boldsymbol{b}(t)^T}{\phi_t}\right]\right)^{-1}$$

Refer to section B of the appendix for computations.

3.2.2 Full conditional for hyperparameters Y_j

The full conditional density of our j-*th* kernel-specific hyperparameters is of the form

$$f(Y_j|Z_j) \propto H(Z_j|Y_j)\mathcal{L}(Y_j) \tag{23}$$

As above, for simplicity of notation, we drop the index j that denotes the kernel membership, keeping in mind that any full conditional is for the hyperparameters of the j-*th* group.

Full conditional for hyperparameters of $\boldsymbol{\mu}$

We recall that we set the following hyperprior structure $(\boldsymbol{m_0},\ \Lambda_0) \sim \text{NIW}(\boldsymbol{\theta_0}, k_0, \nu_0, \Delta_0)$. Moreover, we recall that $H(\boldsymbol{\mu}|\boldsymbol{m_0}, \Lambda_0) \overset{law}{=} \mathcal{N}(\boldsymbol{m_0}, \Lambda_0)$. Hence we have that the full conditional law is

$$\mathcal{L}(\boldsymbol{m}_0, \Lambda_0|\boldsymbol{\mu}) \propto \mathcal{N}(\boldsymbol{\mu}; \boldsymbol{m}_0, \Lambda_0) \times \text{NIW}(\boldsymbol{m}_0, \Lambda_0; \boldsymbol{\theta_0}, k_0, \nu_0, \Delta_0)$$

Since the normal-inverse-Wishart structure is conjugate with the normal distribution, we have that

$$\boldsymbol{m}_0, \Lambda_0|\boldsymbol{\mu} \sim \text{NIW}(\boldsymbol{\theta_1}, k_1, \nu_1, \Delta_1)$$

where

$$k_1 = k_0 + 1 \qquad \nu_1 = \nu_0 + 1$$

$$\boldsymbol{\theta_1} = \frac{k_0\ \boldsymbol{\theta}_0 + \boldsymbol{\mu}}{k_1}$$
$$\Delta_1 = \Delta_0 + \frac{k_0}{k_1}(\boldsymbol{\mu} - \boldsymbol{\theta}_0)(\boldsymbol{\mu} - \boldsymbol{\theta}_0)^T$$

3.3 Sample in logarithmic scale

In Step 2 of the Blocked Gibbs sampler, we would like to sample from a categorical distribution. It is worth noticing that the probabilities of the categorical distribution are proportional to the likelihood (25). The evaluation of the likelihood in the different atoms of the different kernels requires the product of a high number factors. To better control this number, avoiding it attains values less than the machine ϵ, we compute this number in logarithmic scale. This means that, instead of $(p_1, \ldots, p_N)$ we have $(\log(p_1), \ldots, \log(p_N))$. In order to obtain the probabilities and to sample, we apply the following transformation:

$$p_k = \frac{1}{\sum_{j=1}^{N} \exp(\log(p_j) - \log(p_k))} = \frac{\exp(\log(p_k))}{\sum_{j=1}^{N} \exp(\log(p_j))}, \tag{24}$$

It is noteworthy that the transformation works up to a translation on the logarithm scale, i.e defining $\log(p_j^*) = \log(p_j) + C$.

In our particular case, we have that for observation i

$$f(\boldsymbol{X}_i|Z_j, Y_j) = \prod_{t=t_0}^{T} \frac{1}{\sqrt{2\pi\phi_{jt}}} \exp\left\{-\frac{(X_i(t) - \mu_j(t))^2}{2\phi_{jt}}\right\} \tag{25}$$

so that

$$\log f(\boldsymbol{X}_i|Z_j, Y_j) = \sum_{t=t_0}^{T} \left[-\frac{1}{2}\log(2\pi\phi_{jt}) - \frac{(X_i(t) - \mu_j(t))^2}{2\phi_{jt}}\right]$$

Hence, we have

$$p_{j,i} = p_j \cdot f(X_i|Z_j, Y_j)$$

then

$$\log p_{j,i} = \log(p_j \cdot f(X_i|Z_j, Y_j)) = \log(p_j) + \sum_{t=t_0}^{T} \left[-\frac{1}{2}\log(2\pi\phi_{jt}) - \frac{(X_i(t) - \mu_j(t))^2}{2\phi_{jt}}\right].$$

3.4 Parameters elicitation

The parameters to elicitate are those of the hyperpriors of $\boldsymbol{\mu}$, the mass α of the Dirichlet process and the parameters c and d of the inv-gamma prior of ϕ_t.

3.4.1 Hyperparameters

We proceed using our data for the elicitation of the parameters of the hyperprior. We recall we set a normal-inverse-Wishart structure on our data and referring to the notation of section 2.3 the parameters to elicitate are $\boldsymbol{\theta_0}$, κ_0, ν_0 and Δ_0.
First, we set the expected value of $\boldsymbol{\mu_0}$ equal to the empirical mean of the coefficients of the considered data with respect to the basis expansion, that is

$$\boldsymbol{\theta_0} = \mathbb{E}[\boldsymbol{m_0}] = \frac{1}{n}\sum_{i=1}^{n}\boldsymbol{\beta}_i$$

Second, the expected value of Λ_0 is set equal to the empirical variance of the coefficients of the considered data with respect to the basis expansion, keeping ν_0 the lowest possible we get

$$\nu_0 = L$$
$$\mathbb{E}[\Lambda_0] = \frac{\Delta_0}{\nu_0 - L + 1} = \frac{1}{(n-1)}\sum_{i=1}^{n}(\boldsymbol{\beta}_i - \bar{\boldsymbol{\beta}})^2$$

Finally, κ_0 is set equal to 0.1, in order to increase the variance of $\boldsymbol{m_0}$, so to allow the algorithm to propose more flexible values of the coefficients of $\boldsymbol{\mu}$.

3.4.2 Mass

As far as the mass is concerned, at first we set it such that the number of expected clusters is equal to desired value; that is, for instance

$$\mathbb{E}\left[K_n\right] = \sum_{i=1}^{n}\frac{\alpha}{\alpha + j - 1} = 3 \iff \alpha \simeq 0.6$$

Since in such setting the algorithm performs very poorly in terms of mixing, allowing for much higher values of mass turns out to be very effective in obtaining a better mixing. Therefore, we test the algorithm with $\alpha \simeq 40$.

3.4.3 Prior for ϕ_t parameters

The setting of the parameters of the inv-gamma prior for ϕ_t has been particularly critical. We see that the most effective elicitation comes as result of a sort of trade-off between mixing performance of the algorithm and its ability to separate observations in clusters. Eventually, we see that the best performance is obtained by setting c and d such that

$$\mathbb{E}[\phi_t] = \frac{d}{c-1} = 1 \quad \text{and} \quad \mathrm{Var}(\phi_t) = \frac{d^2}{(c-1)^2(c-2)} = 0.2$$

which is reasonable, since we do not want ϕ_t to be so high that a curve could be assigned to a cluster that is not representative of it, and on the contrary we do not want ϕ_t to be so small that it becomes very difficult to propose a value of μ that generates a new cluster.

4 Simulated data

In order to assess performances of the specified model, we simulate data from three distinct Gaussian Processes, aiming at separating them in three clusters.

4.1 Uncorrelated time points

For each of the three groups, we generate $n = 10$ data $X_i(t)$, $(i = 1, ..., n$ and $t = 1, ..., T)$ on a grid of $T = 100$ time points, according to $X_i(t)|\boldsymbol{\mu}_i, \{\phi_{it}\}_t \overset{ind}{\sim} GP(\mu_i, R_i)$, specifying a sinusoidal mean function $\mu(t)$ and a covariance operator $R(t, t')$ coherent with our model: $R(t, t') = \begin{cases} \phi_t & \text{if } t = t' \\ 0 & \text{if } t \neq t' \end{cases}$, where we simulate ϕ_t from an inverse gamma distribution. In particular the mean operator of the three groups are sinus functions with

1. amplitude= 0.55, angular frequency= 0.2π, phase= 0
2. amplitude= 0.2, angular frequency= 0.2π, phase= 0.4
3. amplitude= 0.55, angular frequency= 0.35π, phase= 1.4

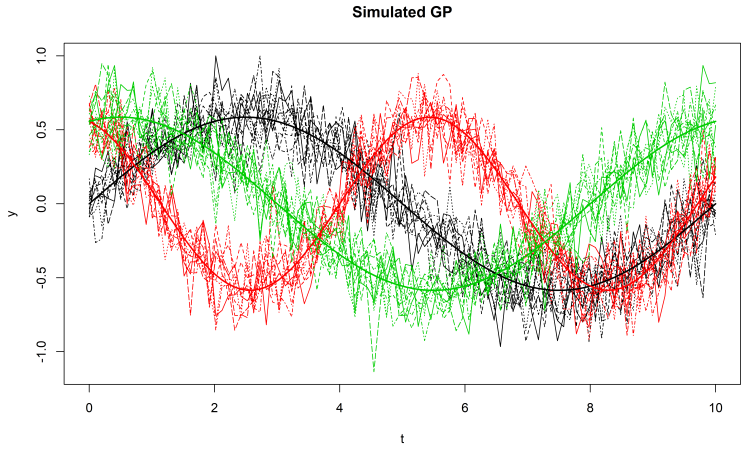

Figure 1: Simulated data with diagonal covariance matrix

In Figure 1 we report simulated data from the three Gaussian processes.
In the framework of dimensionality reduction (see Section 2.1), we have to select an appropriate number of basis functions to represent our data. Since we are using periodic data, a natural choice is to truncate the basis system to 7 basis functions, that allows to capture 3 harmonic frequencies.

4.2 Exponential covariance function

It is noteworthy that the previous data construction does not violate the assumption of independence between time points. To test the performance of the model in a framework in which this assumption is not met, we simulate again data from three Gaussian processes, considering this time a discretization of an exponential covariance function of the form: $R(t, t') \propto e^{-\beta|t'-t|}$ over a 1D grid $[t_1, \ldots, t_T]$, thus obtaining the PxP covariance

matrix of values: $R_{i,j} = C(t_i, t_j) \propto e^{-\beta|t_i - t_j|}$.
In Figure 2 we report simulated data from the three Gaussian processes, with correlated times.

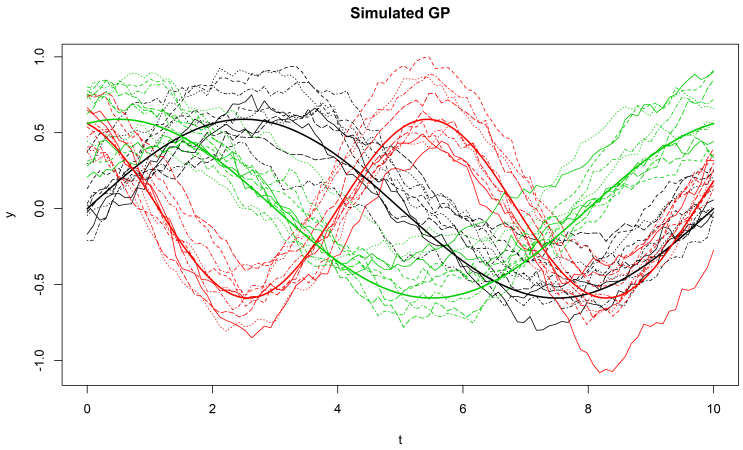

Figure 2: Simulated data with exponential covariance matrix

4.2.1 Testing on GP with uncorrelated time points

We ran posterior sampling for 5000 iterations after 10000 burnin iterations. Trucation level of stick breaking prior is fixed at 500.
By minimizing Binder loss function, optimal allocation of observations separates data into three groups, leading to perfect clustering of simulated data.
In Figure 3b we report posterior similarity matrix.
In Figure 3a we report traceplots of cluster allocation variables K_i for some observations i.
We can appreciate good mixing and standard diagnostic tests like Geweke test showed no evidence against convergence of the chain.

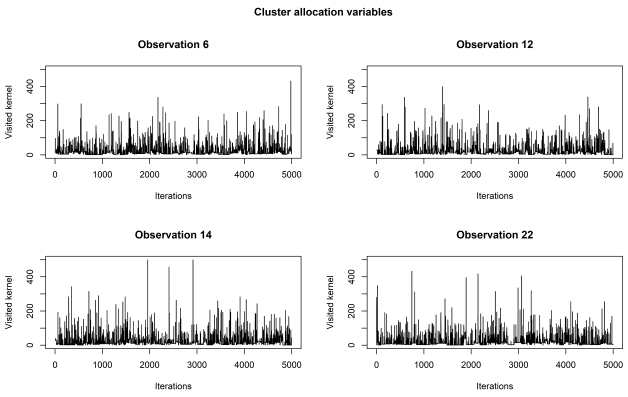

(a) Traceplots of cluster allocation variables

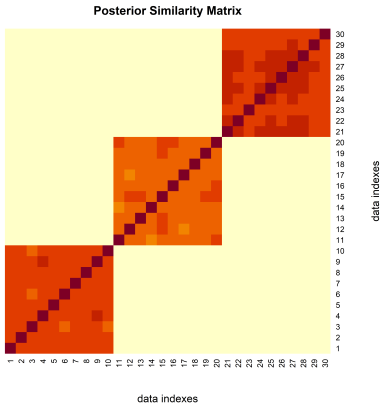

(b) Posterior Similarity Matrix

Figure 3: Traceplots and PSM for simulated data

4.2.2 Testing on GP with correlated time points

Posterior inference is again performed for 5000 iterations after 10000 burnin iterations. Trucation level of stick breaking prior is fixed at 500. Despite the presence of a positive correlation within times, the algorithm is still able to propose suitable kernels and performances are not worsen.
In Figure 4b we report the posterior similarity matrix.
In Figure 4a we report traceplots of cluster allocation variables.

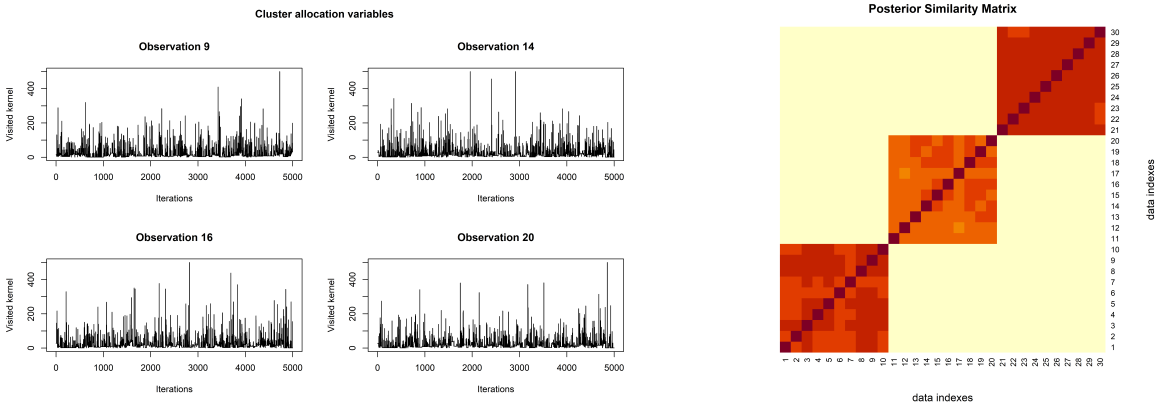

(a) Traceplots of cluster allocation variables

(b) Posterior Similarity Matrix

Figure 4: Traceplots and PSM for simulated data

5 Clinical data

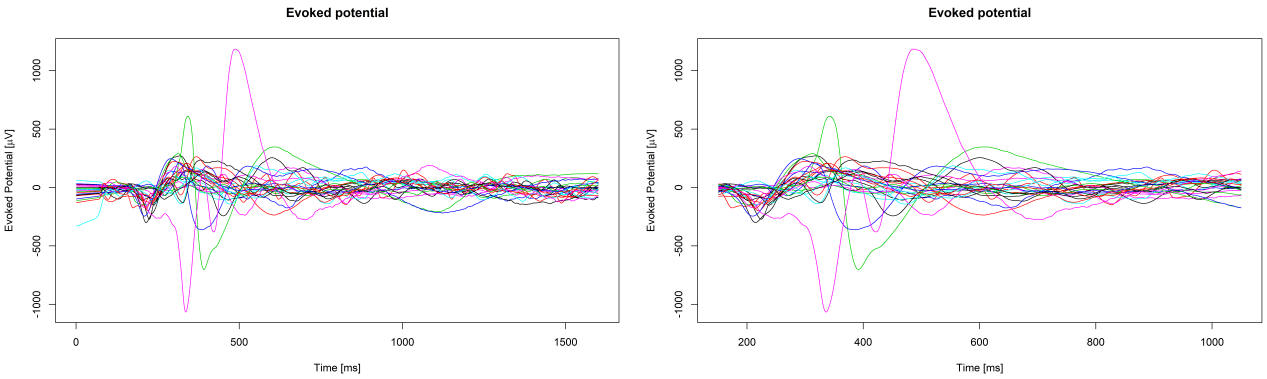

(a) Original signal

(b) Cutted signal

Figure 5: Left lobe short latency signal

5.1 Data cleaning and basis expansion

First, we proceed cleaning our data. In figure 5a, we observe that our functions present long tails. We decide to focus on the central and most shape-characteristic part of our functions, keeping the points from the 150^{th} to the 1500^{th} (see figure 5b). Furthermore, due to computational reasons, we decide to keep one time point out

of nine, getting finally *100* time points.
On the other hand, in the context of dimensionality reduction (see Section 2.1), we opted for a regression splines approach for smoothing. We set the spline order of the spline basis to *4* and the number of the basis is chosen through a generalized cross validation criterion (GCV) (see Ramsay and Silverman 2005). We compute the GCV index for each function over a grid of possible number of basis (from *6* to *80*) and then compute the mean for each possible number of basis over the different functions. The minimum value of the mean of the GCV index is attained for 80 basis, but we can appreciate from fig 6 that around 25 basis there is an elbow. We hence opt for a fourth-order spline basis of 25 basis functions.
Finally, we re-scale our data, dividing by the maximum value attained by all the observations.

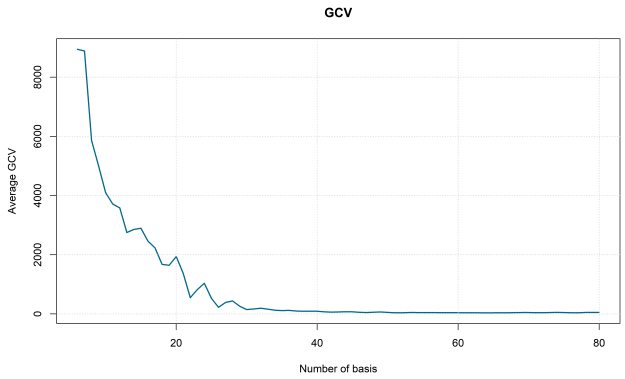

Figure 6: Mean of GCV index over the different functions for different possible number of basis

5.2 Testing

We run the algorithm for 5,000 iterations after 15,000 of burnin. The truncation level of the stick-breaking sampler set to 500.
The mixing of the algorithm is very good, as we may notice from the traceplots of the cluster allocation of observations. Nonetheless, the posterior similarity matrix clearly shows how the algorithm is reluctant in separating observations in different clusters. We notice that only 1 out of 26 observations are separated from the others in the partition that minimizes the Binder loss function. Being this curve the most different in terms of range suggests that the algorithm is not really able to distinguish between the others.
In Figure 7a we report traceplots of cluster allocation variables.
In Figure 7b we report the posterior similarity matrix.
In Figure 8 we report the functional observations, coloring them by mean of the optimal partition.

This interpretation of the previous inference is confirmed by many tests conducted on the same set of function without that observation, since the algorithm is still unable to separate the curves.

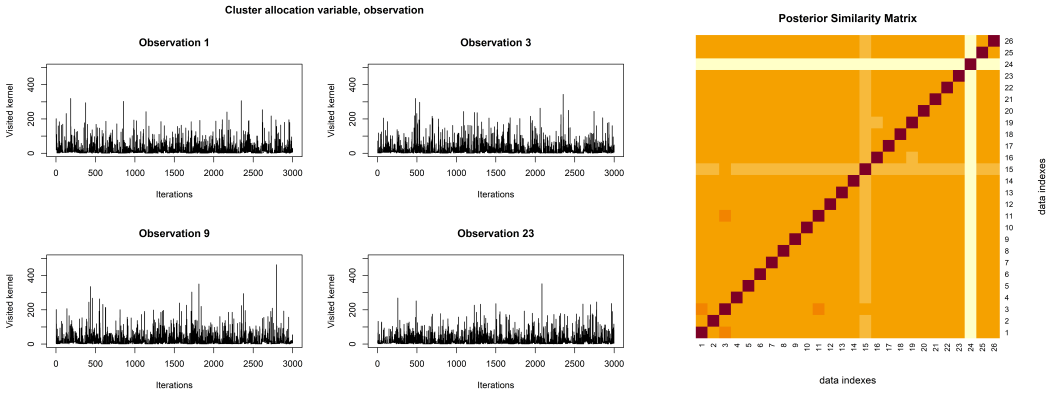

(a) Traceplots of cluster allocation variables

(b) Posterior similarity matrix

Figure 7: Left lobe short latency signal: traceplots and PSM

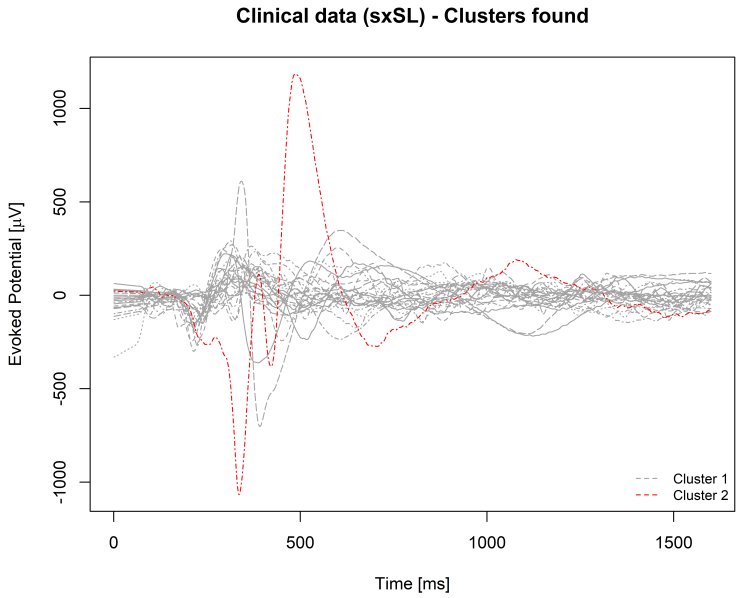

Figure 8: Left lobe short latency signal: clusters found

We repeat the analysis on all four components of the Sensorial Evoked Potential, observing the algorithm perform in a similar way. That is, it is only able to isolate the curves that are clearly different in terms of amplitude and phase with respect to the others.
We report here posterior inference for the right lobe short latency (dxSL) signal, in Figure 9a we report traceplots of cluster allocation variables.
In Figure 9b we report the posterior similarity matrix.
In Figure 10 we report the functional observations, coloring them by mean of the optimal partition.

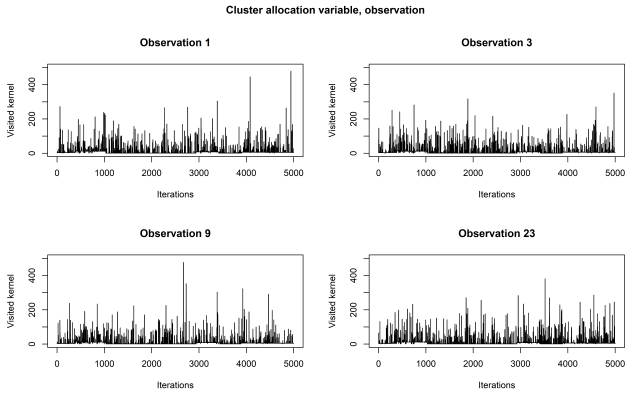

(a) Traceplots of cluster allocation variables

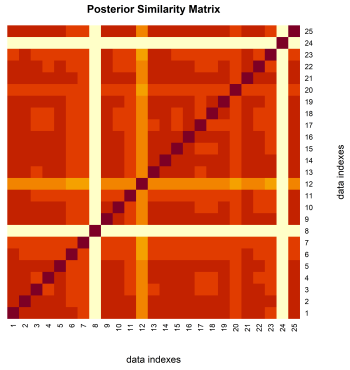

(b) Posterior similarity matrix

Figure 9: Right lobe short latency signal: traceplots and PSM

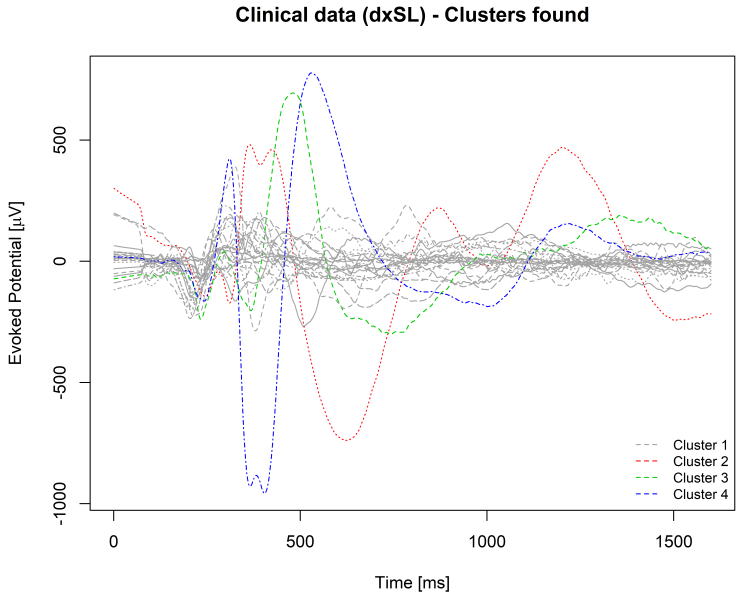

Figure 10: Right lobe short latency signal: clusters found

5.2.1 Proposal of a new model

Given such poor performance in the clustering of observations, we extend the model by dropping the assumption of identical distribution for the ϕ_t $\forall t$. Namely, we now assume $\forall t$:

$$\phi_t \overset{ind}{\sim} IG(c_t, d_t)$$

We implement a new sampling algorithm accordingly and test it both on simulated data and on our observations. Since the testing of the algorithm do not result in any improvement in the clustering performance, we decide to mention this extension only in this subsection, and not to give it any more emphasis.

5.3 Conclusions

The proposed algorithm has not been able to perform an effective clustering of clinical data. In particular, in all the four components no clustering structure is detected, except for the isolation of very dissimilar functions in shape and amplitude. We argue that this may be due to different reasons. First, our model may not be adequate for our real data. In particular, our data may be far from being effectively modeled by mixture of Gaussian Processes, especially with our assumptions on the form of the covariance operator. A possible research path may be to set a more complex form of the covariance operator, dropping for instance the assumption of independence between different time instants. On the other hand, a more complex hyperprior structure may be set, as done in Scarpa and Dunson 2014, where also a hyperprior is set on the parameters of the inv-gamma prior on ϕ_t (12). This has not been done for different reasons, among whom the problem of the absence of conjugacy that leads to the need of a Metropolis-Hastings step in the algorithm. The computation of the acceptance rate as in ibid. would have required the product of high number of factors that may lead to very low acceptance probabilities and so to increase substantially the computation time.

A Full conditional for ϕ_t

Fix $t \in \{t_0, \dots, T\}$, we have

$$f(\phi_t|\text{rest}) \propto H(\phi_t) \prod_{\{i:K_i=j\}} f(X_i(t)|Z_j, Y_j).$$

We recall that prior for ϕ_t is $\forall t\ \phi_t \overset{iid}{\sim} IG(c,d)$.
Hence we have

$$\begin{aligned} f(\phi_t|\text{rest}) &\propto (\phi_t)^{-c-1} e^{-d/\phi_t} \prod_{\{i:K_i=j\}} (\phi_t)^{-1/2} \exp\left\{-\frac{(X_i(t)-\mu(t))^2}{2\phi_t}\right\} \\ &\propto (\phi_t)^{-c-1} e^{-d/\phi_t} (\phi_t)^{-r/2} \exp\left\{-\frac{1}{\phi_t} \sum_{\{i:K_i=j\}} \frac{(X_i(t)-\mu(t))^2}{2}\right\} \\ &\propto (\phi_t)^{-(c+r/2)-1} \exp\left\{-\frac{1}{\phi_t}\left[d + \sum_{\{i:K_i=j\}} \frac{(X_i(t)-\mu(t))^2}{2}\right]\right\} \end{aligned}$$

We finally have

$$\phi_t|\text{rest} \sim \text{inv-gamma}\left(c + \frac{r}{2}, d + \sum_{\{i:K_i=j\}} \frac{(X_i(t)-\mu(t))^2}{2}\right)$$

B Full conditional for $\boldsymbol{\mu}$

We have

$$f(\boldsymbol{\mu}|\text{rest}) \propto H(\boldsymbol{\mu}|Y_j) \prod_{\{i:K_i=j\}} f(\mathbf{X}_i|Z_j, Y_j)$$

For what concerns the first term, we recall that the prior for $\boldsymbol{\mu}$ is $\boldsymbol{\mu}|\boldsymbol{m_0}, \Lambda_0 \sim \mathcal{N}_L(\boldsymbol{m_0}, \Lambda_0)$.
We now want to express the likelihood of X_i in terms of $\boldsymbol{\beta}_i$, the vector of coefficients of the projection in basis.
We exploit the basis expansion introduced in 2.1, in particular we recall that

$$X_i(t) = \boldsymbol{b}(t)^T \cdot \boldsymbol{\beta}_i \qquad \mu(t) = \boldsymbol{b}(t)^T \cdot \boldsymbol{\mu}$$

This allows us to rewrite the density of $\mathbf{X}_i|Z_j, Y_j$ in the following way

$$\begin{aligned} f(\mathbf{X}_i|Z_j, Y_j) &\propto \prod_{t=t_0}^{T} \exp\left\{-\frac{(X_i(t)-\mu(t))^2}{2\phi_t}\right\} \\ &\propto \exp\left\{-\frac{1}{2}\sum_{t=t_0}^{T} \frac{(X_i(t)-\mu(t))^2}{\phi_t}\right\} \\ &\propto \exp\left\{-\frac{1}{2}\sum_{t=t_0}^{T} \frac{(\boldsymbol{b}(t)^T\boldsymbol{\beta}_i - \boldsymbol{b}(t)^T\boldsymbol{\mu})^2}{\phi_t}\right\} \\ &\propto \exp\left\{-\frac{1}{2}(\boldsymbol{\beta}_i - \boldsymbol{\mu})^T \sum_{t=t_0}^{T} \frac{\boldsymbol{b}(t)\boldsymbol{b}(t)^T}{\phi_t}(\boldsymbol{\beta}_i - \boldsymbol{\mu})\right\} \end{aligned}$$

We have that the full conditional for μ is of the form

$$f(\boldsymbol{\mu}|\text{rest}) \propto \mathcal{N}_L(\boldsymbol{m_0}, \Lambda_0) \prod_{\{i:K_i=j\}} f(\mathbf{X}_i|Z_j)$$

$$\propto \exp\left\{-\frac{1}{2}(\boldsymbol{\mu}-\boldsymbol{m}_0)^T\Lambda_0^{-1}(\boldsymbol{\mu}-\boldsymbol{m}_0)\right\} \prod_{\{i:K_i=j\}} \exp\left\{-\frac{1}{2}(\boldsymbol{\beta}_i-\boldsymbol{\mu})^T \sum_{t=t_0}^{T} \frac{\boldsymbol{b}(t)\boldsymbol{b}(t)^T}{\phi_t}(\boldsymbol{\beta}_i-\boldsymbol{\mu})\right\}$$

If we consider the argument of the exponentials, dropping $-\frac{1}{2}$ and setting $B := \sum_{t=t_0}^{T} \frac{\boldsymbol{b}(t)\boldsymbol{b}(t)^T}{\phi_t}$ we obtain

$$(\boldsymbol{\mu}-\boldsymbol{m}_0)^T\Lambda_0^{-1}(\boldsymbol{\mu}-\boldsymbol{m}_0) + \sum_{\{i:K_i=j\}} (\boldsymbol{\beta}_i-\boldsymbol{\mu})^T B(\boldsymbol{\beta}_i-\boldsymbol{\mu})$$

$$\propto \boldsymbol{\mu}^T\Lambda_0^{-1}\boldsymbol{\mu} - 2\boldsymbol{\mu}^T\Lambda_0^{-1}\boldsymbol{m}_0 + \boldsymbol{\mu}^T \sum_{\{i:K_i=j\}} B\boldsymbol{\mu} - 2\boldsymbol{\mu}^T B \sum_{\{i:K_i=j\}} \boldsymbol{\beta}_i$$

$$\propto \boldsymbol{\mu}^T\left[\Lambda_0^{-1} + rB\right]\boldsymbol{\mu} - 2\boldsymbol{\mu}^T\left(\Lambda_0^{-1}\boldsymbol{m}_0 + B\sum_{\{i:K_i=j\}} \boldsymbol{\beta}_i\right)$$

$$\propto \boldsymbol{\mu}^T\Lambda_r^{-1}\boldsymbol{\mu} - 2\boldsymbol{\mu}^T\Lambda_r^{-1}\Lambda_r\left(\Lambda_0^{-1}\boldsymbol{m}_0 + B\sum_{\{i:K_i=j\}} \boldsymbol{\beta}_i\right)$$

$$\propto (\boldsymbol{\mu}-\boldsymbol{m}_r)^T\Lambda_r^{-1}(\boldsymbol{\mu}-\boldsymbol{m}_r)$$

where

$$\boldsymbol{m}_r = \Lambda_r\left(\Lambda_0^{-1}\boldsymbol{m}_0 + \left[\sum_{t=t_0}^{T} \frac{\boldsymbol{b}(t)\boldsymbol{b}(t)^T}{\phi_t}\right] \sum_{\{i:K_i=j\}} \boldsymbol{\beta}_i\right)$$

$$\Lambda_r = \left(\Lambda_0^{-1} + r\left[\sum_{t=t_0}^{T} \frac{\boldsymbol{b}(t)\boldsymbol{b}(t)^T}{\phi_t}\right]\right)^{-1}$$

Given these calculations, we conclude that the full conditional for $\boldsymbol{\mu}$ is

$$\boldsymbol{\mu}|\text{rest} \sim \mathcal{N}_L(\boldsymbol{m}_r, \Lambda_r) \tag{26}$$

Articles

Ferguson, T.S. (1973). "A Bayesian analysis for some nonparametric problems". In: *The annals of statistics* 1.2, pp. 209–230.

Ishwaran, Hemant and Lancelot F. James (2001). "Gibbs sampling methods for stick-breaking priors". In: *Journal of the American Statistical Association* 96.453, pp. 161–173.

Neal, Radford M. (2000). "Markov chain sampling methods for Dirichlet process mixture models". In: *Journal of Computational and Graphical Statistics* 9.2, pp. 249–265.

Scarpa, Bruno and David B. Dunson (2014). "Enriched stick-breaking processes for functional data". In: *Journal of the American Statistical Association* 109.506, pp. 647–660.

Teh, Y. W (2010). "Dirichlet processes". In: *Encyclopedia of Machine Learning, Springer*.

Books

Mueller, P. et al. (2015). *Bayesian Nonparametric Data Analysis*. Springer.

Ramsay, J. and B. Silverman (2005). "Functional Data Analysis". In: Springer. Chap. 4.

Software

R Core Team (2013). "R: A Language and Environment for Statistical Computing". In: URL: http://www.R-project.org/.

R-packages

David Kahle, James Stamey (2017). "invgamma: The Inverse Gamma Distribution". In: URL: https://CRAN.R-project.org/package=invgamma.

Fritsch, Arno (2012). "mcclust: Process an MCMC Sample of Clusterings". In: URL: https://CRAN.R-project.org/package=mcclust.

Hadley Wickham Jim Hester, Winston Chang (2015). "devtools: Tools to Make Developing R Packages Easier". In: URL: https://CRAN.R-project.org/package=devtools.

Ieva, Francesca et al. (2019). "roahd Package: Robust Analysis of High Dimensional Data". In: *The R Journal* 11.2, pp. 291–307. URL: https://doi.org/10.32614/RJ-2019-032.

J. O. Ramsay Spencer Graves, Giles Hooker (2020). "fda: Functional Data Analysis". In: URL: https://CRAN.R-project.org/package=fda.

Kevin Kuang Quyu Kong, Francesco Napolitano (2019). "pbmcapply Package: Tracking the Progress of Mc*pply with Progress Bar". In: URL: https://cran.r-project.org/web/packages/pbmcapply/index.html.

Meschiari, Stefano (2015). "latex2exp Package: Use LaTeX Expressions in Plots". In: URL: https://CRAN.R-project.org/package=latex2exp.

Plummer, Martyn et al. (2006). "CODA: Convergence Diagnosis and Output Analysis for MCMC". In: *R News* 6.1, pp. 7–11. URL: https://journal.r-project.org/archive/.

Statisticat and LLC. (2020). "LaplacesDemon: Complete Environment for Bayesian Inference". In: R package version 16.1.4. URL: https://web.archive.org/web/20150206004624/http://www.bayesian-inference.com/software.

Venables, W. N. and B. D. Ripley (2002). "Modern Applied Statistics with S". In: ISBN 0-387-95457-0. URL: https://www.stats.ox.ac.uk/pub/MASS4/.

Wade, Sara (2015). "mcclust.ext: Process an MCMC Sample of Clusterings". In: URL: https://github.com/sarawade/mcclust.ext.

Wickham, Hadley (2011). "The Split-Apply-Combine Strategy for Data Analysis". In: *Journal of Statistical Software* 40.1, pp. 1–29. URL: http://www.jstatsoft.org/v40/i01/.

Github repository for the code

(N.d.). URL: https://github.com/Niccolo-Ajroldi/Functional-BNP-clustering.